



ELSEVIER

Journal of Chromatography A, 910 (2001) 347–357

JOURNAL OF
CHROMATOGRAPHY A

www.elsevier.com/locate/chroma

Dual effect of high electric field in capillary electrophoresis study of the conformational stability of *Bungarus fasciatus* acetylcholinesterase

Daniel Rochu^{a,*}, Thierry Pernet^a, Frédérique Renault^a, Cassian Bon^b, Patrick Masson^a

^aUnité d'Enzymologie, Centre de Recherches du Service de Santé des Armées, B.P. 87, 38702 La Tronche Cedex, France

^bUnité des Venins, Institut Pasteur, 75724 Paris Cedex 15, France

Received 29 May 2000; received in revised form 28 November 2000; accepted 28 November 2000

Abstract

The effect of high electric field in capillary zone electrophoresis (CZE) was evaluated for the study of the thermally induced unfolding of *Bungarus fasciatus* acetylcholinesterase. This monomer enzyme is characterised by two interdependent uncommon structural features, the asymmetrical distribution of charged residues and a relatively low thermal denaturation temperature. Both traits were presumed to interfere in the thermal unfolding of this enzyme as investigated by CZE. This paper analyses the effect of high electric field on the behaviour of the enzyme native state. It is shown that increasing the applied field causes denaturation-like transition of the enzyme at a current power which does not induce excessive Joule heating in the capillary. The susceptibility to electric field of proteins like cholinesterases, with charge distribution anisotropy, large permanent dipole moment and notable molecular flexibility associated with moderate thermal stability, was subsequently discussed. © 2001 Elsevier Science B.V. All rights reserved.

Keywords: *Bungarus fasciatus*; Protein folding; Acetylcholinesterase; Cholinesterase; Enzymes

1. Introduction

Acetylcholinesterase (AChE, EC 3.1.1.7) plays a critical role in cholinergic transmission [1]. As well as butyrylcholinesterase (BuChE, EC 3.1.1.8), AChE is inhibited by organophosphates (OPs) used as pesticides, medicines, and potent chemical warfare agents [2]. Engineering of cholinesterases (ChEs) to make catalytic bioscavengers for detoxification of OP compounds [3] is a new promising research field. Surprisingly, soluble monomer AChE is abundant in

the venom of the snake *Bungarus fasciatus* [4,5]. Glycosylation-related microheterogeneity [5], sensitivity to inhibitors and to peripheral site ligands [6] and influence of the electric dipole moment of the protein on the traffic of substrates and products in the catalytic gorge have been analysed [7]. Active *Bungarus* AChE produced in transfected COS cells was secreted about 30 times more efficiently than an equivalent secreted monomeric rat AChE [6]. In addition, the snake enzyme has a turnover number ($\approx 390\,000\text{ min}^{-1}$ with acetylthiocholine at pH 7.4) clearly higher than those of *Torpedo* and mammalian ChEs [8]. Thus, the *Bungarus* AChE should be a useful template for designing catalytic bioscavengers of OP compounds.

*Corresponding author. Tel.: +33-4-7663-6964; fax: +33-4-7663-6961.

E-mail address: rochudan@compuserve.com (D. Rochu).

The core of capillary electrophoresis (CE) is the use of a narrow electrophoresis channel that enables quick dissipation of heat and allows the application of a high field strength. Although CE analysis of proteins is particularly difficult, due primarily to the propensity of proteins to bind on the capillary wall, successful CE resolutions of proteins were achieved. One way to prevent wall interactions is the use of high-ionic-strength buffers [9], resulting in high current that generates heat. Meanwhile, commercially available CE apparatuses generally fulfil the conditions required for controlling heat generation and heat dissipation.

Recently we described a capillary zone electrophoresis (CZE) approach with optimised temperature control for studying thermal stability of proteins at various pH [10,11]. This method allowed the thermodynamic parameters of bovine β -lactoglobulin thermal denaturation to be estimated. The goal of the present work was to use CZE for investigating the thermal stability of *Bungarus* AChE. The information are expected to be useful for designing OP-degrading mutant ChEs with improved catalytic efficiency and increased structural stability. In this report, we exploit CE to attempt at a characterisation of the thermal unfolding of *Bungarus* AChE. Due to the anisotropic distribution of electric charges of the enzyme, and its relatively low denaturation temperature, several problems must have been solved. Finally, even if CE systems are equipped with efficient temperature control devices, their ability to allow analysis of native proteins is discussed.

2. Experimental

2.1. Materials

Bungarus fasciatus venom collected in Cambodia was from the stock of Institut Pasteur (Paris, France). Venom AChE was purified by affinity chromatography as previously described [5]. Reagents of analytical grade were from Sigma (L'Isle d'Abeau, France). *N,N*-Dimethylformamide (DMF) used as a marker for electroosmotic flow (EOF) determination was from Pierce (Rockford, IL, USA). All buffer and wash solutions were prepared in Milli-Q water (Millipore, Waltham, MA, USA) and filtered through

disposable 0.45- μ m filters (Schleicher & Schuell, Dassel, Germany).

2.2. Protein characterisation and assays

Homogeneity of purified *Bungarus* AChE was checked by sodium dodecyl sulfate–polyacrylamide gel electrophoresis and isoelectric focusing (IEF) on PhastGel (pH range 4–6.5; Pharmacia, Uppsala, Sweden). The isoelectric point (pI) was determined using a pI protein calibration kit (Pharmacia). Electrophoretic titration curve analysis was carried out by IEF on Phastgel on the wide pH range (3–9). Experimental titration curve was compared to the theoretical titration curve built using ABIM, a software resident on the ExPaSy server (<http://www.ex-pasy.ch>). Proteins were stained with Coomassie brilliant blue, or with silver nitrate. Non-denaturing gels were stained for AChE activity according to Karnovsky and Roots [12]. AChE activity was determined using the method of Ellman et al. [13]. Protein concentration in highly purified enzyme preparations was determined using the bicinchoninic acid method (Pierce) with bovine serum albumin as the standard.

2.3. Instrumentation and electrophoretic procedure

A Beckman P/ACE 5500 CE system (Fullerton, CA, USA), with P/ACE Station software was used throughout this study. Bare fused-silica capillaries (50 μ m I.D.) of different length were housed in a liquid-thermostated cartridge. For precise temperature control up to 95°C, the CE apparatus was modified and equipped with a thermocouple microprobe implanted inside the cartridge, as previously described [10]. Capillary and autosampler tray with samples and buffer vials were thermostated separately using two circulating baths.

CE was operated with the usual polarity (sample injected at the anode), at a constant applied voltage. Electrophoresis was carried out at different temperatures, over the temperature range of approximately 20–60°C. The protein samples (1 mg ml⁻¹), maintained at 20°C before analysis, were co-injected with DMF (0.01%, v/v, final concentration) hydrodynamically by overpressure (3.45 kPa). The dura-

tion of injection was decreased (2% °C⁻¹) to correct for the decrease in viscosity with increasing temperature. After each run, the capillary was flushed with running buffer (five capillary volumes). Acquisition of absorbance data in the range 195–300 nm was performed using the diode array device. Electropherograms showed absorbance at a single wavelength (200 nm).

2.4. Analysis of electrophoretic data and of thermal unfolding profiles

Mobilities and thermodynamic parameters associated with unfolding transitions were calculated through the software from the apparent migration times and the area under the curves, respectively. The mobility of AChE was calculated as follows:

$$\mu = \mu_{\text{app}} - \mu_{\text{eo}} = \frac{L_t L_d}{V} \cdot \left(\frac{1}{t_{\text{app}}} - \frac{1}{t_{\text{eo}}} \right) \quad (1)$$

where μ , μ_{app} and μ_{eo} represent the electrophoretic, apparent and electroosmotic mobility (cm² V⁻¹ s⁻¹), respectively. L_t is the total length of the capillary and L_d the length of the capillary from inlet to detector. V stands for the applied voltage, t_{app} for the apparent migration time and t_{eo} for the migration time of the EOF marker.

Individual values of μ were plotted against the temperature to determine the unfolding transition profile of *Bungarus* AChE under different buffer conditions. Surfaces of overlapping peaks were fitted after deconvolution using PeakFit software (SPSS Science, Chicago, IL, USA). Mid-transition temperature (T_m) was determined by two methods: (a) $T_{m,\mu}$ was estimated following thermally-induced mobility change. μ data for *Bungarus* AChE, calculated according to Eq. (1), resulted in a sigmoidal transition when plotted as a function of T . The profile was characterised by linear pre- and post-transition regions, reflecting the mobility characteristics of the native (N) and unfolded (U) protein species, respectively. In the transition region, the non-linearity was attributed to size and charge changes occurring upon unfolding. $T_{m,\mu}$ corresponds to the temperature at the inflexion point of the sigmoid curve; (b) $T_{m,vH}$ was determined assuming N and U in equilibrium, by direct UV quantitation of CE peaks. Areas under the

curves allow calculation of relative concentrations of the two enzyme populations. A van 't Hoff analysis of the unfolding transition was possible by fitting the relative peak areas to relation:

$$\ln K_D = f(1/T), \text{ with } K_D = [U]/[N] \quad (2)$$

3. Results and discussion

3.1. Method development and CE analysis of thermal unfolding of *Bungarus* AChE

When analysing proteins by CE, one of the major problems encountered is the adsorption of proteins on the fused-silica capillary wall because of ionic, hydrophobic, and/or other weak interactions [14,15]. Thus, the choice of a good buffer system is of the utmost importance. The buffer must be tailored to the characteristics of the protein; it must fulfil the two essential prerequisites, optimal separation, and preservation of the molecular integrity of the protein to be analysed. The protein pI is an important parameter to take into account. Although in some cases it is possible to estimate pI from the titration curve as built from the protein amino acid composition, experimental determination of pI is more reliable. Titration curve analysis was carried out to evaluate the electrophoretic behaviour of the enzyme as a function of pH of the buffers to be used in CE. As seen in Fig. 1, *Bungarus* AChE exhibits glycosylation-related charge microheterogeneity and a very shallow titration curve in the pH 6 to 9 side. Although pH > 9 is theoretically beneficial for CE runs because of the maximum net charge of AChE, alkaline conditions were shown to considerably enhance the resolution of glycoforms. Our first goal was to carry out the study of thermal unfolding of native AChE, providing a single homogeneous migration peak. Thus, phosphate buffer, with small ionisation heat, was preferred to borate buffer, which is known for its ability to resolve glycoforms. In addition, since high-ionic-strength buffers are efficient for minimising protein adsorption, 0.1 M sodium phosphate buffers were used as running electrolytes.

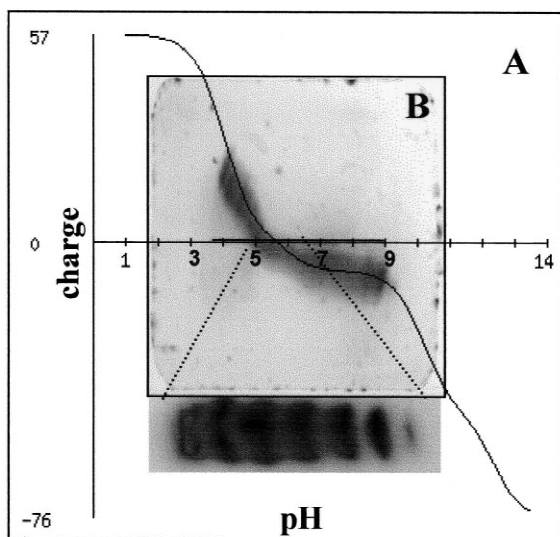


Fig. 1. Theoretical (A) and experimental (B) titration curves of *Bungarus* AChE in the pH ranges 1–13 and 3–9, respectively. Inset: microheterogeneity of AChE as seen in IEF gel in the pH range 5–6.5.

We were prompted to evaluate the thermal stability of the snake AChE. CE migrations were thus conducted using the phosphate buffer at pH 7.3, at different temperatures between 20 and 50°C. A temperature of 50°C was the upper limit for CZE analysis without clogging the capillary by denatured AChE aggregates. Fig. 2A displays representative electropherograms for the EOF marker and AChE. An additional peak appeared above 30°C, and its area increased with temperature up to 50°C. Plots of electrophoretic mobility (not shown), and fraction of unfolded protein (Fig. 2B) versus the temperature (T), showed mid-transition temperatures ($T_{m,\mu}$ and $T_{m,vH}$) values of ~ 41 and 39.8°C, respectively. $T_{m,\mu}$ was estimated with low accuracy. Indeed, the decrease in mobility was too steep in the transition region to provide enough values for drawing the sigmoid denaturation curve using graphical softwares. Validity of the two-state and reversibility assumptions for *Bungarus* AChE are discussed below.

The kinetics of thermal inactivation of *Bungarus* AChE was previously studied between 45 and 54°C [16]. A significant irreversible thermal denaturation

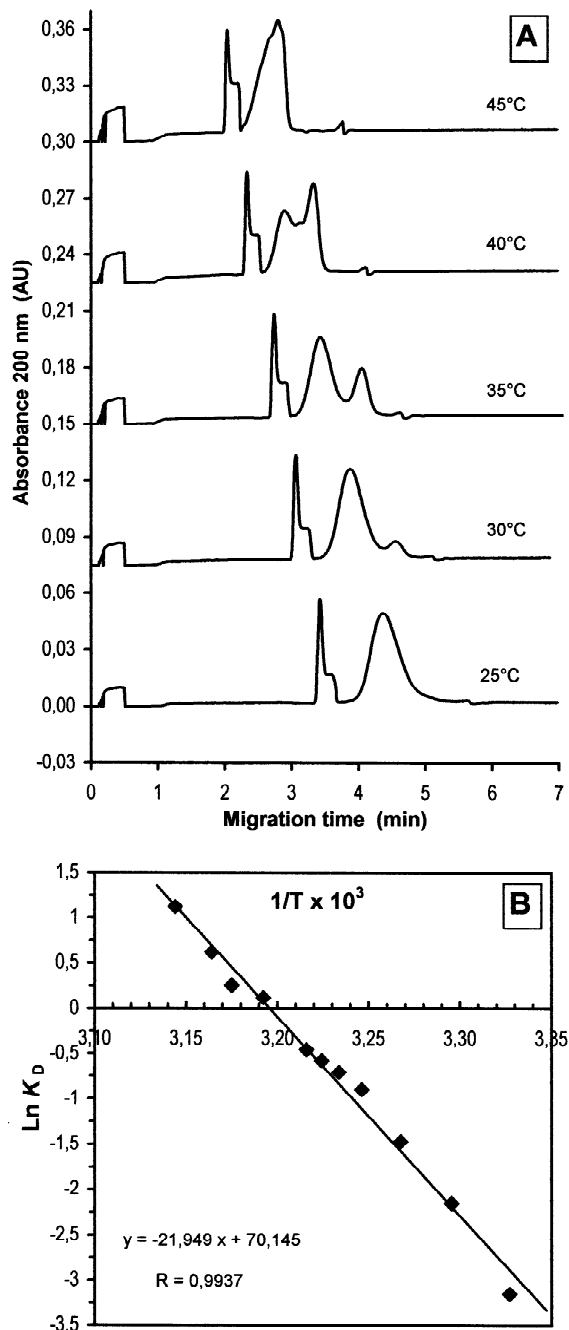
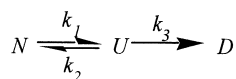


Fig. 2. (A) Typical electropherograms for *Bungarus* AChE between 25 and 45°C. The sample and run buffer was 100 mM sodium phosphate, pH 7.3, electrophoresis was conducted at 10 kV in a 27 cm \times 50 μ m capillary and detection was set at 200 nm. The first peak corresponds to DMF (the EOF marker), and the others to AChE. (B) van 't Hoff plot ($\ln K_D$ vs. $1/T$) for the native and unfolded populations of AChE estimated using PeakFit by area under the curves.

was observed with half-life ~ 90 min at 45°C . The heat-denatured enzyme was shown to aggregate rapidly and $>99\%$ of the enzyme was inactivated after 5 min at 53°C . Finally, it was proposed that the thermal denaturation of *Bungarus* AChE obeys first-order kinetics. Irreversible thermal denaturation of human BuChE [17,18] and AChE [19] and of *Torpedo* AChE [20] is well documented. In particular, denaturation was studied by differential scanning microcalorimetry (DSC). This technique is widely used to investigate the thermodynamics of protein folding–unfolding transitions. However, analysis of calorimetric data in terms of the equilibrium formalism requires reversibility of the unfolding process [21,22]. However, numerous proteins do not fulfil this requirement and their denaturation is kinetically controlled due to an irreversible step [23]. Such a process under kinetic control can be described by the Lumry and Eyring model [24]:



where N is the native state, U is an unfolded form and D the final denatured state, k_{obs} the first-order rate constant:

$$k_{\text{obs}} = \frac{k_3}{1 + \frac{1}{K_U}} \text{ with } K_U = \frac{[U]}{[N]} = \frac{k_1}{k_2} \quad (3)$$

There are no available data for thermal denaturation of *Bungarus* AChE using DSC. In our work, denaturation study using CE was beforehand considered, assuming a priori an irreversible process leading to aggregation of the protein, as DSC measurements showed for other cholinesterases (Table 1). Using CE, any populated molecular state detected as a migrating peak is assumed to correspond to a soluble form. Accordingly, non-native peaks whose intensity is increasing with temperature can reflect the formation of unfolded (non-denatured) U protein states. For DSC measurements, it was found that at high scan rates ($\geq 1.5^\circ\text{C min}^{-1}$), there is no significant dependence of the heat capacity on the scan rate, indicating that equilibrium models may be used for computation of DSC data [26]. In our technique, protein samples, maintained at 20°C before injection, migrated for about 3 min in the capillary thermostated between 38 and 44°C , i.e., temperatures corresponding to the denaturation transition region. This corresponds to scan rates $>6\text{--}8^\circ\text{C min}^{-1}$. Under such conditions, $k_3 \ll k_2$ in Eq. (3), and

Table 1
Thermodynamic parameters available for the thermally induced denaturation of cholinesterases from different species

Enzyme	Reversible	T_m^a ($^\circ\text{C}$)	E_A (kJ mol^{-1})	ΔH_{cal} (kJ mol^{-1})	ΔH_{vH} (kJ mol^{-1})	$\Delta H_{\text{cal}}/\Delta H_{\text{vH}}$	ΔC_p^d ($\text{kJ mol}^{-1} \text{K}^{-1}$)	$\Delta C_p^{\text{theor}^b}$ ($\text{kJ mol}^{-1} \text{K}^{-1}$)	Refs.
Human BuChE (tetramer)	No	63.3	325	3230	890	3.6	37.4 ^c	36.7	[17,18]
Human rAChE (dimer)	No	59.2	450	1500	600	2.5	42.3	37.4	[19]
<i>Torpedo</i> AChE (dimer)	No	45	548	1600				34.0	[20]
<i>Bungarus</i> AChE (monomer)	No		470 431					37.4	[16] _d

^a DSC scan rate = 1°C min^{-1} .

^b $\Delta C_p^{\text{theor}}$: theoretical values (italicised) estimated according to the relation by Myers et al. [25]: $\Delta C_p^{\text{theor}} = 4.184 \cdot 10^{-3} [-172 + (17.6N) - (164SS)]$ (in $\text{kJ mol}^{-1} \text{K}^{-1}$), based on information from the structure of the protein (N, number of amino acid residues; SS, number of disulfide bridges in the protein).

^c P. Masson et al., unpublished.

^d V.L. Shnyrov, I. Silman, C. Bon, L. Weiner, manuscript in preparation.

therefore, the transition temperature can be considered as insensitive to the scan rates [25]. Accordingly, the equilibrium thermodynamics formalism can be applied to the analysis of CE data.

3.2. Heat dissipation during CE of *Bungarus* AChE

When repeating experiments to estimate the reproducibility of the method, we observed T_m values ranging from 36 to 41°C. Moreover, the value of determined van 't Hoff enthalpy change (ΔH_{vH}) associated with the denaturation transition was inaccurate due to the poor resolution of the N and U forms. Consequently, further runs were conducted at higher voltages to improve peak resolution. Surprisingly, although the AChE sample and the capillary were both thermostated at 20°C, unfolding-like transitions occurred as the voltage increased (Fig. 3). To prevent erroneous interpretation of this phenomenon, a thorough examination of the physicochemical characteristics of both the CE conditions and *Bungarus* AChE molecule was carried out. In other words, we tried to establish whether the transitions observed were either thermally-induced, i.e., due to a failure to dissipate excessive Joule heating in the capillary, or field-induced. Joule heating results from the current intensity developed in buffers by high electric fields. Fortunately, for properly thermostated capillary, the radial difference in temperature between the buffer and the capillary wall is $\leq 1^\circ\text{C}$ when a power of 7 W m^{-1} is applied [27]. Effective thermostating devices, using forced liquid cooling, were found mandatory for a variety of applications where powers as high as 5 to 7 W m^{-1} can be generated [28,29]. Likewise, high-ionic-strength buffers such as 0.5 M phosphate, providing up to 3 W m^{-1} in $20 \mu\text{m}$ I.D. capillaries, were recommended for separation of proteins [9]. The temperature difference between the different material interfaces of a fused-silica capillary is described by:

$$T_c - T_a = \frac{EI}{2\pi} \cdot \left(\frac{1}{2k_b} + \frac{1}{k_s} \cdot \ln \frac{r_2}{r_1} + \frac{1}{k_p} \cdot \ln \frac{r_3}{r_2} + \frac{1}{r_3 h} \right) \quad (4)$$

where T_c is the temperature at the centre of the capillary and T_a the temperature of the surroundings;

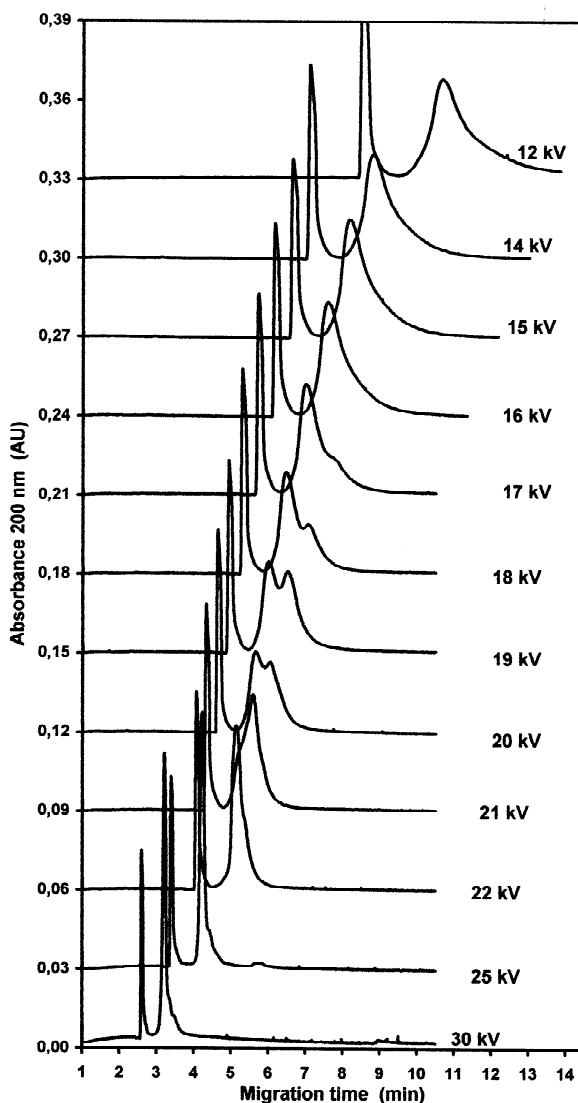


Fig. 3. Capillary electropherograms at 20°C of *Bungarus* AChE obtained using 100 mM phosphate buffer at pH 7.3 in a $47 \text{ cm} \times 50 \mu\text{m}$ fused-silica capillary, 12 to 30 kV potential, and 200 nm detection. The faster peak is DMF, and the other peaks are AChE forms.

r_1 , r_2 and r_3 are the radii of the open channel, the silica wall and the polymer coating, respectively; k_b , k_s and k_p are the thermal conductivities of the buffer, silica and the polymer, respectively; h is the heat transfer coefficient.

The CE apparatus uses a liquid cooling system for thermostating; it is equipped with a thermocouple

microprobe introduced within the cartridge close to the capillary wall. This device was a priori validated to provide efficient dissipation of Joule heating. To check this assumption, voltage-dependence of both electroosmotic velocity and current intensity (Ohm's law) were plotted. The first plot is indicative for the control of the double layer temperature. The second one reflects the effectiveness of the thermal dissipation between the capillary outer wall and the cooling medium around the capillary. As shown in Fig. 4, both plots were linear for voltage up to 20 kV with correlation coefficient greater than 0.99, indicating that the temperature in the capillary was constant in this range of applied voltage. In addition, to prevent the stacking phenomenon susceptible to generate heat in the sample plug, both the sample and run buffers were at the same concentration (0.1 M). Consequently, thermally-induced denaturation of *Bungarus* AChE at 20°C by deficient heat dissipation was not demonstrated.

3.3. Field strength effects on unfolding of *Bungarus* AChE

Studies of polyelectrolyte conformation changes induced by high electric fields, were extensively devoted to nucleic acids [30]. Although the effects of

electric fields on globular proteins are more difficult to investigate, numerous studies were reported [31]. Two major field-induced changes in macromolecules can be distinguished. The first one is the rotational motion of molecules with dipole moments, moving their dipole vector into the direction of the field vector. The second one is conformational changes resulting from displacement of ionised protein side chains. Often regarded as completely separate phenomena, field-induced orientation effects and field-induced reaction effects are related [31]. Studies on bovine serum albumin [32] and haemoglobin [33,34] demonstrated that electric parameters of proteins are as variable as their structure, and thus that general statement is hardly possible. Nevertheless, field-induced changes seen with these proteins did not lead to denaturation.

Dipole moments of several hundred debyes appear to be standard among proteins, whereas dipole moments higher than 1000 D are less common [35]. It is noteworthy that *Bungarus* AChE was found to bear a permanent electric dipole moment in the range of about 1000 D, as experimentally determined by electrooptical measurements [7]. A dipole of similar magnitude was previously calculated for the *Torpedo californica* AChE dimer [36,37]. The large dipole moment of AChEs was thought to increase their efficiency by directing the cationic substrates to the active site via a deep and narrow gorge [36], and a recent study discerned a ionic surface trap and an ionic strength-dependent electrostatic steering mechanism in ChEs [38]. This corroborates and refines the biological significance of the singular surface charge distribution and the associated macrodipole of these enzymes. Moreover, the dynamics of the AChE electrostatic field was described [39] (see also <http://chemcca10.ucsd.edu/dache/>), showing potential fluctuations on the order of 50% around the "southern" hemisphere (away from the gorge).

Bacteriorhodopsin was shown to undergo an intramolecular conformational change induced at a relatively low electric field of $\approx 150 \text{ V cm}^{-1}$ [40]. Although bacteriorhodopsin and AChE are unrelated proteins, convergent functional features exist. Bacteriorhodopsin is a patch-organised protein involved in ion transport across the bacterial membrane. The middle-sized dipole moments ($\sim 570 \text{ D}$) associated with each protein molecule add up to huge moments

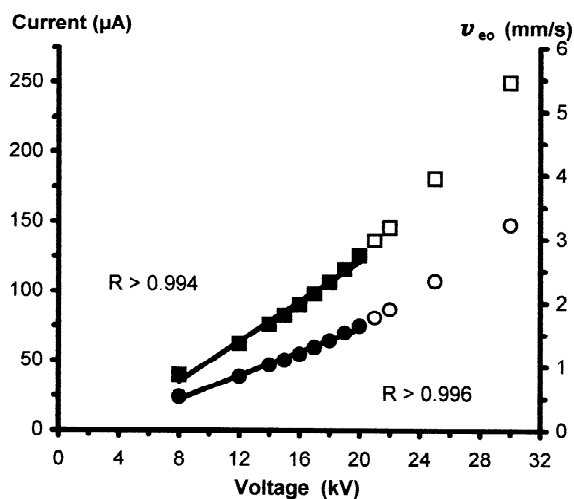


Fig. 4. Voltage dependence of electroosmotic velocity (left y-axis, squares), and Ohm's law plot (right y-axis, circles) for migrations in the voltage range 8–30 kV; linear fitting concerned closed symbols.

(several 10^6 D) for the whole patch [35]. Although *Bungarus* AChE is a soluble monomeric enzyme with a dipole moment of ~ 1000 D, and has no known function, the main physiological role of AChEs is to terminate transmission at cholinergic synapses by rapid hydrolysis of the neurotransmitter, ACh. For this, AChE is highly concentrated at the neuromuscular junction (up to 3000 molecules per μm^2 of postsynaptic area [41]). Besides, different types of synapses display different repertoires of molecular forms of AChE [1], this in turn reflecting strict requirements for spatial distribution and/or orientation of AChE at a given synapse [42].

In other respects, most of the lengthy α -helices and β -sheets in AChE have overall orientations matching with the gorge axis and the dipole direction (Fig. 5). When submitted to high electric field, such an oriented configuration could enable a destructive molecular stretching, similar to field-induced helix-coil transitions described for polypeptides like poly-L-lysine, and for single-strand polynucleotides [30,31]. The topology of the majority of long β -sheets in the “northern-southern” axis could pro-

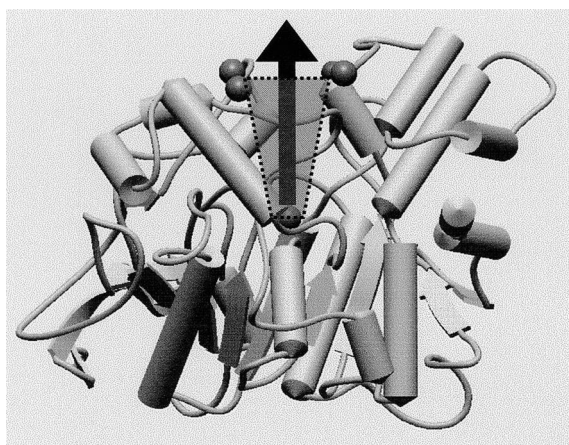


Fig. 5. Schematic ribbon representation of the *Bungarus* AChE model, built using the SwissModel automatic modelling server from ExPASy, with the coordinates of PDB entry 1ace (*Torpedo* AChE) and the amino acid sequence of *Bungarus* AChE. The rim and the bottom of the active site gorge (grey truncated cone) are indicated, from left to right, by CB of S 277(280), CA of T 70(73), O of I 330(333), CG of K 282(285), and by CD of I 441(444), respectively (*Bungarus* AChE numbering, the *Torpedo* AChE numbering follows in parentheses). The arrow indicates direction of the dipole.

mote the unfolding process by a sliding mechanism similar to the force-induced extension of proteins as studied by atomic force microscopy (AFM) [43]. It is noteworthy that: (a) an AFM study of *Torpedo* AChE immobilised by the positive end of its dipole with the negative end left free, showed images suggesting that enzyme molecules have been widened, (i.e., flattened) due to their elasticity [44]; (b) in situ IR spectroscopy study of *Torpedo* AChE showed different orientation of α -helix and β -sheet components relatively to the compression at the air-water interface [45]. Accordingly, the possibility of physically-induced reversible or irreversible deformations of AChE, along a preferential axis, cannot be ruled out.

Finally, as far as we are aware, the incidence of the electric field in CE on the behaviour of proteins having large dipole moments has not yet been investigated. Only in the case of a rod-shaped protein particle (tobacco mosaic virus, TMV) submitted to CZE, it was noted that electric field from 175 to 400 V cm^{-1} was strong enough to make orientation effects worth considering (by induced moment caused by polarisation of the counterion atmosphere immediately adjacent to the TMV particle) [46]. Orientation effect and the Wien effect are known to be able to increase mobility of molecules. In the case of AChE, these effects were unlikely. Indeed, the quasi-spherical shape of *Bungarus* AChE cannot account for an orientation effect, and the Wien effect was described for fields in the order of 10^5 V cm^{-1} [47]. Moreover, the electrophoretic mobility of *Bungarus* AChE did not increase with \vec{E} during CE (Fig. 3). On the contrary, a transition towards a molecular form exhibiting slower mobility was observed above a field of 300 V cm^{-1} . Accordingly, a role of electrostatic shielding associated with a huge permanent dipole moment showing weak dependence on the ionic strength, on the susceptibility of the monomeric snake AChE to undergo a conformational change by stretching when submitted to electric field strength higher than 300 V cm^{-1} , was found to be a possibility.

Other interesting facts were observed for *Bungarus* AChE using 20 to 100 mM phosphate as run buffer, 10 to 30 kV as applied voltage and 5 to 20°C as capillary thermostating temperature (Fig. 6). Peak broadening and additional peaks, resulting from electrostatic interactions between AChE and silica

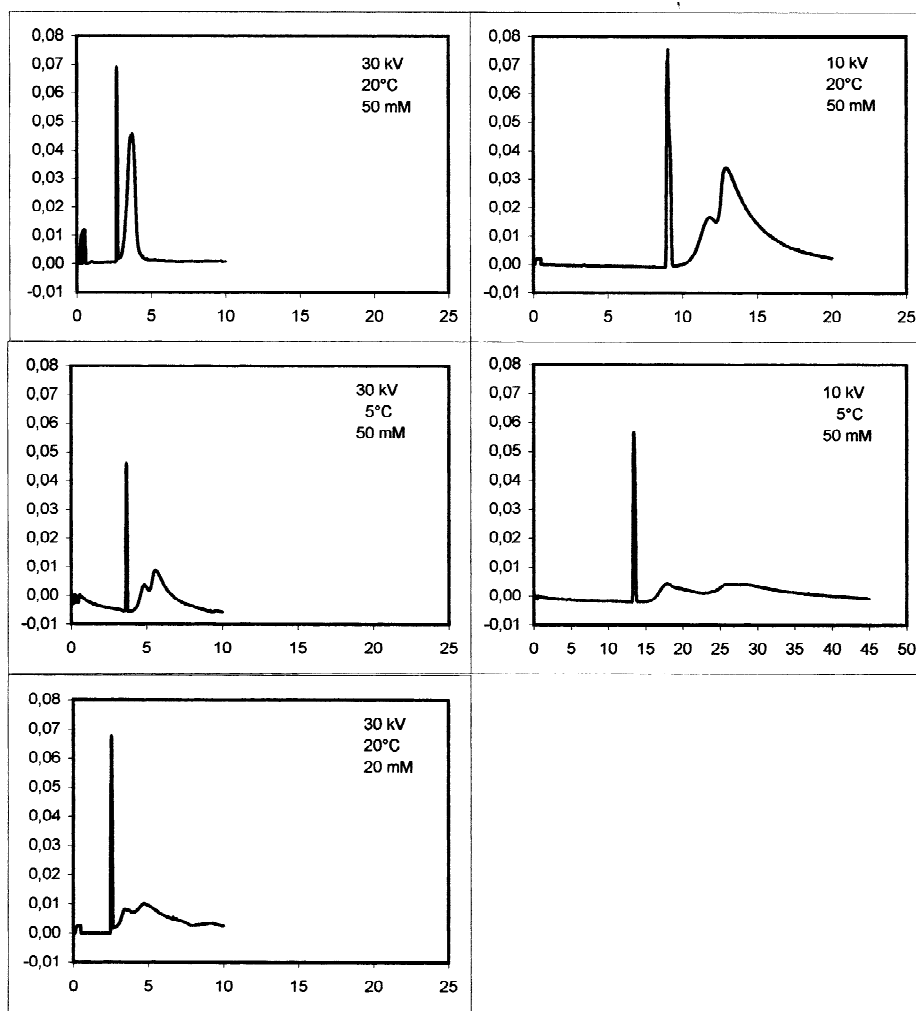


Fig. 6. Effect of applied voltage, temperature and ionic strength of run buffer, on peak shape of *Bungarus* AChE. Left column, 30 kV; right column, 10 kV; upper and lower rows, 20°C; middle row, 5°C; the two upper rows, 50 mM; lower row, 20 mM. x-Axis, migration time (min); y-axis, absorbance 200 nm (mAU). Wall interaction decreased as voltage, temperature and ionic strength increased.

wall were observed in some conditions. Interactions were favoured by lowering the temperature at constant voltage, by lowering the applied voltage at constant temperature, or by lowering the buffer ionic strength at constant temperature and voltage. In addition, uncoated capillaries have charged inner walls capable of interacting with proteins at pH > 2. When used in the neutral to basic pH range, they generate substantial electroosmotic flow in the direction of the cathode. At the same time, the snake AChE having a negative net charge and an

asymmetrical repartition of charged residues is forced to migrate in the opposite direction. Altogether the above-mentioned features were capable of interfering, rendering in turn difficult to describe the real behaviour of *Bungarus* AChE in CE when the electric field is higher than 300 V cm^{-1} . New investigations must be planned to substantiate the likelihood of field-induced conformational change of proteins such as ChEs, exhibiting a large dipole moment and a conformational plasticity. In keeping with these two special features can be recalled the

extreme effectiveness of these catalysts (the “perfect enzymes”), acting at rates that are almost diffusion controlled [48]. The intrinsic instability of enzymes may be the underlying mechanism that provides the necessary structural flexibility for a protein to adapt its three-dimensional structure in response to the binding of a ligand. Accordingly, because our main objective was the study of the thermal stability of *Bungarus* AChE, further CE analysis were conducted using limited field strength and Joule heating. Under these very cautious conditions, the T_m and ΔH of the unfolding transition were estimated and confirmed the moderate thermal stability of the enzyme (D. Rochu et al., BBA, in press).

4. Conclusions

The CZE study of a monomeric AChE, having a large permanent dipole moment and characterised by a low unfolding temperature, allowed to unveil several crucial facts. The use of high-ionic-strength buffer essential to prevent wall interactions, resulted in elevated current susceptible to generate excessive Joule heating. Screening of the CE system characteristics as well as examination of the experimental conditions used, provided valuable information which would moderate the optimistic general belief asserting that CE performances, including analysis of protein samples, are satisfactory for applied power up to 5 W m^{-1} . Notwithstanding, this survey failed to denote either an inadequate temperature control or a badly dissipated Joule heating in the capillary used to analyse the thermal stability of *Bungarus* AChE. On the other hand, the occurrence of a “denaturation-like” transition at 20°C for runs carried out at high electric field strength, suggests a possible field-induced conformational change of this enzyme. One of the future prospects of CE is the micro-miniaturisation of apparatuses, allowing the use of extremely high electric fields (5000 V cm^{-1}) [49]. Using such tools, further study should lead to more insight into the combined effects of electric field, ionic strength, viscosity, electroosmosis on the CZE behaviour of flexible proteins displaying large dipole moments.

Acknowledgements

We would like to thank Bernard Saliou (Unité des Venins, Institut Pasteur, Paris, France) for enzyme purification and Beckman-Coulter France (Division Biorecherche), for facilitating the modification of the P/ACE instrument. This work was supported by grant No. 99 CO 029/PEA 990802 from DSP/STTC to P.M.

References

- [1] J. Massoulié, L. Pezzementi, S. Bon, E. Krejci, F.-M. Vallette, *Prog. Neurobiol.* 44 (1993) 31.
- [2] B. Ballantyne, T.C. Marrs, *Clinical and Experimental Toxicology of Organophosphates and Carbamates*, Butterworth/Heinemann, London, 1992.
- [3] C.B. Millard, O. Lockridge, C.A. Broomfield, *Biochemistry* 37 (1998) 237.
- [4] V. Kumar, W.B. Elliott, *Eur. J. Biochem.* 34 (1973) 586.
- [5] X. Cousin, C. Créminon, J. Grassi, K. Méflah, G. Cornu, B. Saliou, S. Bon, J. Massoulié, C. Bon, *FEBS Lett.* 387 (1996) 196.
- [6] X. Cousin, S. Bon, N. Duval, J. Massoulié, C. Bon, *J. Biol. Chem.* 271 (1996) 15099.
- [7] D. Pörschke, C. Créminon, X. Cousin, C. Bon, J. Sussman, I. Silman, *Biophys. J.* 70 (1996) 1603.
- [8] Y. Frobort, C. Créminon, X. Cousin, M.-H. Rémy, J.-M. Chatel, S. Bon, C. Bon, J. Grassi, *Biochim. Biophys. Acta* 1339 (1997) 253.
- [9] F.T. Chen, J.C. Sternberg, *Electrophoresis* 15 (1994) 13.
- [10] D. Rochu, G. Ducret, P. Masson, *J. Chromatogr. A* 838 (1999) 157.
- [11] D. Rochu, G. Ducret, F. Ribes, S. Vanin, P. Masson, *Electrophoresis* 20 (1999) 1586.
- [12] M.J. Karnovsky, L. Roots, *J. Histochem. Cytochem.* 12 (1964) 219.
- [13] G.L. Ellman, K.D. Courtney, V. Andreas, R.M. Featherstone, *Biochem. Pharmacol.* 7 (1961) 88.
- [14] J.J. Bonvent, R. Barbieri, R. Bartolino, L. Capelli, P.G. Righetti, *J. Chromatogr. A* 756 (1996) 233.
- [15] F.E. Regnier, D. Wu, in: N.A. Guzman (Ed.), *Capillary Electrophoresis Technology*, Marcel Dekker, New York, 1993.
- [16] I. Shin, I. Silman, C. Bon, L. Wiener, *Biochemistry* 37 (1998) 4310.
- [17] P. Masson, S. Rey, C. Cléry, N. Fontaine, C. Kronman, B. Velan, A. Shafferman, in: USAMRICD (Ed.), *Bioscience Review*, Vol. 1, published by the USA Medical Research Institute of Chemical Defense, 1996, p. 43.
- [18] P. Masson, C. Cléry, P. Guerra, A. Redtslob, C. Albaret, P.-L. Fortier, *Biochem. J.* 343 (1999) 361.

- [19] M. Lebleu, C. Cléry, P. Masson, S. Reuveny, D. Marcus, B. Velan, A. Shafferman, in: D.M. Quinn, A.S. Balasubramanian, B.P. Doctor, P. Taylor (Eds.), *Enzymes of the Cholinesterase Family*, Plenum Press, New York, 1995, p. 131.
- [20] D.I. Kreimer, V.L. Shnyrov, E. Villar, I. Silman, L. Weiner, *Prot. Sci.* 4 (1995) 2349.
- [21] P.L. Privalov, *Adv. Prot. Chem.* 33 (1979) 167.
- [22] J.M. Sturtevant, *Annu. Rev. Phys. Chem.* 38 (1987) 463.
- [23] J.M. Sanchez-Ruiz, *Biophys. J.* 61 (1992) 921.
- [24] R. Lumry, H. Eyring, *J. Phys. Chem.* 58 (1954) 110.
- [25] J.K. Myers, N.C. Pace, J.M. Scholtz, *Prot. Sci.* 4 (1995) 2138.
- [26] J.W. Tanner, R.G. Eckenhoff, P.A. Liebman, *Biochim. Biophys. Acta* 1430 (1999) 46.
- [27] J.R. Veraart, C. Gooijer, H. Lingeman, *Chromatographia* 44 (1997) 129.
- [28] R.J. Nelson, A. Paulus, A.S. Cohen, A. Guttman, B.L. Karger, *J. Chromatogr.* 480 (1989) 111.
- [29] R.J. Nelson, D.S. Burgi, in: J.P. Landers (Ed.), *Handbook of Capillary Electrophoresis*, CRC Press, Boca Raton, FL, 1994, p. 549.
- [30] D. Pörschke, *Biopolymers* 15 (1976) 1917.
- [31] D. Pörschke, *Annu. Rev. Phys. Chem.* 36 (1985) 159.
- [32] C.L. Riddiford, B.R. Jennings, *J. Am. Chem. Soc.* 88 (1966) 4359.
- [33] G. Ilgenfritz, T.M. Schuster, in: B. Chance, T. Yonetani, A.S. Mildvan (Eds.), *Probes of Structure and Function of Macromolecules and Membranes*, Academic Press, New York, 1971, p. 299.
- [34] J. Antosiewicz, D. Pörschke, *Biophys. J.* 68 (1995) 655.
- [35] D. Pörschke, *Biophys. Chem* 66 (1997) 241.
- [36] D.R. Ripoll, C.H. Faerman, P.H. Axelsen, I. Silman, J.L. Sussman, *Proc. Natl. Acad. Sci. USA* 90 (1993) 5128.
- [37] J. Antosiewicz, M. K Gilson, I.H. Lee, J.A. McCammon, *Biophys. J.* 68 (1995) 62.
- [38] S.A. Botti, C.E. Felder, S. Lifson, J. Sussman, I. Silman, *Biophys. J.* 77 (1999) 2430.
- [39] S.T. Wlodek, T. Shen, J.A. McCammon, *Biopolymers* 53 (2000) 265.
- [40] D. Pörschke, *Biophys. J.* 71 (1996) 3381.
- [41] L. Angliser, J. Eichler, M. Szabo, B. Haesazert, M.M. Salpeter, *J. Neurosci. Methods* 81 (1998) 63.
- [42] R. Arnon, I. Silman, R. Tarrab-Hazdai, *Prot. Sci.* 8 (1999) 2553.
- [43] T.E. Fisher, A.F. Oberhauser, M. Carrion-Vazquez, P.E. Marszalek, J.M. Fernandez, *Trends Biochem. Sci.* 24 (1999) 379.
- [44] Y. Zhang, D. Zhao, C. Bai, C. Wang, *Life Sci.* 65 (1999) 253.
- [45] L. Dziri, B. Desbat, R.M. Leblanc, *J. Am. Chem. Soc.* 121 (1999) 9618.
- [46] P.D. Grossman, D.S. Soane, *Anal. Chem.* 62 (1990) 1592.
- [47] H.S. Harned, in: H.S. Harned, B.B. Owens (Eds.), *Physical Chemistry of Polyelectrolytes*, 2nd ed., Reinhold, New York, 1950, p. 95.
- [48] D.M. Quinn, *Chem. Rev.* 87 (1987) 955.
- [49] J.P. Landers, T.C. Spelsberg, in: J.P. Landers (Ed.), *Handbook of Capillary Electrophoresis*, CRC Press, Boca Raton, FL, 1994, p. 594.